Bilateral double site (calvarial and mandibular) critical-size bone defect model in rabbits for evaluation of a craniofacial tissue engineering constructs

S. Kotagudda Ranganath, Matthias Schlund, Jérôme Delattre, Joel Ferri, F. Chai

Materials Today Bio 14 (2022) 100267

Contents lists available at ScienceDirect

Materials Today Bio

journal homepage: www.journals.elsevier.com/materials-today-bio

Bilateral double site (calvarial and mandibular) critical-size bone defect model in rabbits for evaluation of a craniofacial tissue engineering constructs

S. Kotagudda Ranganath [a], M. Schlund [a], Jérôme Delattre [c], J. Ferri [a,b], F. Chai [a,*]

[a] Univ. Lille, INSERM, CHU Lille, U1008-Controlled Drug Delivery Systems and Biomaterials, Lille, France
[b] Univ. Lille, INSERM, CHU Lille, Service de Chirurgie Maxillo-Faciale, 2 Avenue Oscar Lambret, Lille, France
[c] Univ. Lille, Univ. Littoral Côte d'Opale, F-62200, Boulogne-sur-Mer, CHU Lille, F-59000, ULR 4490, MABLab - Adiposité Médullaire et Os, Lille, France

ARTICLE INFO

Keywords:
Bone regeneration
Rabbit model
Bone substitute materials
Critical-size defect
Calvaria defect
Mandible defect

ABSTRACT

Most existing preclinical models for evaluating the biosafety and bone-regeneration efficacy of innovative bone substitute materials (BSMs) or tissue engineering (TE) constructs only consisted of a single-site defect and the anatomical locations of defect varied drastically. While the compelling evidence showed that the bone healing pattern is location-dependent, owing to developmental, structural, and functional differences of anatomical locations, this is particularly true for the craniofacial region. Taking this into account, the bone healing efficiency of a BSM shown at one anatomical defect location cannot ensure the same impact at another. This prompted us to develop, for the first time, a model of bilateral critical-sized defect (CSD) at two distinctly different locations (non-load-bearing parietal calvaria and load-bearing mandibular body) co-existing in one rabbit to reduce the number of animals needed and avoid the influence of interindividual variability and evaluation bias on comparisons.

24 healthy adult male New Zealand White rabbits were randomly assigned to a group, either control, autograft (considered the "gold standard") or a clinically relevant BSM (biphasic calcium phosphate granules) (BCPg, Mastergraft®, Medronics). The full-thickness cylindrical calvarial defect (ø10 mm) on frontoparietal region and mandibular composite defect (ø11 mm) on the body of the mandible were created bilaterally using low-speed drilling with saline irrigation. The defect on one side was filled with autograft debris or BCPg, and the other side was no graft (empty). Following the euthanasia of animals at the predetermined intervals (4w and 12w), the defect zones were examined macroscopically and then sampled and processed for microcomputed tomography (microCT) and histological analysis.

All surgeries went uneventfully, and all rabbits recovered slowly but steadily. No symptoms of infection or inflammation associated with the defect were observed during the experiment. At 4w and 12w, macroscopic views of all defect sites were clean without any signs of necrosis or abscess, and no intraoral communication was found. The analysis of microCT and histological findings showed the non-healing nature of the empty defect, thereby both calvaria and mandible CSDs can be validated. The study of the application of BCPg in this defect model highlighted good osteointegration and excellent osteoconductive properties but compromised the osteoinductive properties of this material (compared with autograft).

To conclude, this novel double-site CSD model holds great promise in the application for preclinical evaluation of BSMs, TE construct, etc. With a reduced number of animals in use, and lower interindividual variability and evaluation bias for comparisons.

1. Introduction

In the past 30 years, scientists worldwide have been striving for tissue-engineered (TE) strategies to replace damaged bone. However, only a few of these approaches have made their way into clinical use. "Ideal" preclinical models to evaluate TE constructs are highly needed for filling this gap between research and translation into clinical use/commercialisation [1]. To date, no common guideline for the preclinical

* Corresponding author.
E-mail address: feng.hildebrand@univ-lille.fr (F. Chai).

https://doi.org/10.1016/j.mtbio.2022.100267
Received 14 March 2022; Received in revised form 15 April 2022; Accepted 16 April 2022
Available online 20 April 2022

testing of TE bone constructs exists, although a widely used experimental approach for such study is the "critical size defect" (CSD) model. CSD is defined as a defect that does not heal or, if it does, heals primarily with fibrous tissue and sparse bone within the lifetime of the animal or experiment [2].

Various CSD models have been described for examining bone regeneration in different anatomical regions, which are distinct in their bone healing process due to structural, functional and developmental variations [3,4], such as the long bones [5,6], the skull [7–10], the alveolar bone (maxilla and mandible), etc. [11]. Among them, the parietal calvaria CSD paradigm in rats and rabbits is the most extensively used for evaluating the safety and efficacy of bone tissue constructs, because of its flat shape, non-load-bearing aspect and, subsequently, no need for plates/screws to stabilise the grafts. However, the parietal calvaria bone arises from embryonic paraxial mesoderm cells, while the mandible is derived from the neural crest cells; the latter is known for superior osseous healing capacity compared with that of the mesoderm originated cells (e.g. the calvarial parietal bone) [12,13]. Therefore, the cranial model alone is not only unable to account for the distinct masticatory stress, but also possesses the different cell population from that in the mandibular defect, not to mention other features specific to the mandibular defect, such as soft tissue ingrowth, infectious risk due to the proximity to the oral cavity and the presence of tooth roots [14,15]. All these factors consequently limit its efficiency in the evaluation of novel bone TE constructs [2,16], which are subjected to a combination of considerable mechanical stress. Overall, the calvaria defect model and mandibular alveolar model demonstrate non-load-bearing and load-bearing patterns, respectively, with developmental variations. As a result, there is an obvious benefit to developing a standardised animal model that can effectively evaluate bone tissue constructs at both anatomical locations.

The selection of animal species is another important factor for developing the CSD model. Small (*i.e.* rat, rabbit) and large (*i.e.* dog, sheep, goat, and pig) animals have been described. The latter is advantageous with regard to the dimensions and biomechanical situation, thus, better mimicking the clinical situation, but are time-, labour-, and cost-intensive. The former is more suitable for basic research questions and screening experiments, so, in light of this, mice and rats are the most frequently used species. However, their size limitations and surgical inconveniences, such as limited access to the mandible defect and inability to reach the unique masticatory stress region, make them unreliable for such study. Alternatively, rabbits are a more suitable option with a short breeding cycle, being easy to handle, similar structure and composition to that of human mandibles and a high tolerance for mandible defects [4,17]. In practical terms, the sufficient volume of alveolar bone in the premolar and/or molar areas in rabbits, which allows for developing a suitable mandibular defect [18,19], gives it another advantage as a jawbone CSD model.

The present study aimed at, for the first time, developing a standardised preclinical model with two functionally different (non-load bearing calvarial and load-bearing mandibular) bilateral CSDs in one rabbit, which fairly respects the 3Rs principle by reducing the number of used animals by half in a study. The bilateral calvaria and mandible defects co-existing in one rabbit also avoids interindividual variability and/or evaluation bias and thus, improves the fairness of comparison.

To validate this bilateral double-site CSD model, the "gold standard" autograft was compared to the control (no graft) and the utility of this model was demonstrated by the application of a clinically relevant bone substitute material (biphasic calcium phosphate granules) [7,20,21]. A comprehensive understanding of the benefits/limitations of this new model will potentially aid in the rigorous evaluation of a novel bone substitute material (BSM), TE construct, *etc*.

2. Materials and methods

2.1. Animals and surgery

All experimental animal procedures were carried out at the animal facility at the University of Lille's "Plate-forme Resources Expérimentales - D.H.U.R.E″ in compliance with current European rules for the protection of animals used for scientific reasons (Directive 2010/63/EU). The surgical procedures (no.11664) were reviewed and approved by the local Animal Experimentation Ethics Committee, as well as the French Ministry of Higher Education, Research and Innovation.

24 adult male New Zealand white rabbits, weighing 3.5–4 kg, were evenly distributed into two groups for two graft materials used in this study: "gold standard" autograft (bone debris from defect) and "clinically relevant bone substitute" biphasic calcium phosphate granules (BCPg, 85% β-tricalcium phosphate/15% hydroxyapatite, Mastergraft®, Medtronics, Dublin, Ireland). Each group was then subdivided into two subgroups (6 rabbits per group) and destined to be postoperatively euthanised at two-time points (4 and 12 weeks, respectively). In each rabbit, both the calvarial and the mandibular defects were created bilaterally: the graft (autograft or BCPg) was implanted on one side and no graft (referred to as empty) on the other side ($n = 12$).

Prior to the surgery, for a pre-anaesthetisation antibiotic and analgesic coverage, each animal received a subcutaneous injection of Baytril® (Bayer, Leverkusen, Germany) enrofloxacin solution (5 mg/kg body weight) and an intramuscular injection of analgesic Buprevet® (Virbac France, Carros, France) buprenorphine hydrochloride (0.1 mg/kg body weight). General anaesthesia was induced by intramuscular injections of ketamine hydrochloride (Dechra, Shrewsbury, UK) at 35 mg/kg body weight and xylazine hydrochloride (Randlabs Europe, Ransart, Belgium) at 5 mg/kg body weight and maintained via a V-Gel® supraglottic airway device (Millpledge Veterinary, Nottinghamshire, UK) by delivering a 1.5%–3% isoflurane/O_2 gas mixture. The perimandibular and calvarial parietal areas were subsequently shaved and wiped with Biseptine® (Bayer, Leverkusen, Germany) using sterile gauze.

2.2. Calvaria full-thickness defect

To expose the calvarium, a sagittal midline cranial incision was done with the sterilised #15 scalpel blade. The periosteum was excised to expose the parietal bone. The 10 mm defects were created bilaterally: 2 mm distally to the frontoparietal suture and 2 mm laterally to the midline. Briefly, a bicortical circular osteotomy was performed bilaterally using a dental implant contra-angle handpiece (1:20, SGMS, NSK Europe Ltd., Maidenhead, UK) with a 10 mm trephine bur (#1315/10.0, Medsey srl, Maniago, Italy) operating at 300 rpm with copious saline irrigation. The circular bicortical bone fragment was then gently elevated and luxated with a periosteal elevator without damaging the dura mater. Any remaining debris or bone chips were irrigated gently with sterile saline solution. On one side, the defect was left empty, while on the other side, the defect was filled with BCPg or with bone autograft (morselised bone fragments harvested during the defect creation). Continuous and interrupted stitches of resorbable 3-0 Vicryl sutures (Ethicon®, Johnson & Johnson, Somerville, NJ, USA) were respectively applied to close the overlying soft tissues and skin in layers. The incision was cleaned with Biseptine® using sterile gauze.

2.3. Mandible full-thickness defect

Once the above surgical procedures in calvaria were completed, the animal was positioned in a supine (dorsal) position, via an extraoral approach, an 11 mm defect is created in the molar/premolar region of the

mandible. Briefly, a shallow lateral incision was performed using the #15 scalpel in the inferior mandibular region through fascia and muscle (via an incision through the visible periosteum between the attachment of two muscles on the inferior border), with care taken to detour the facial artery, in order to expose a hemimandible. The defect was positioned anatomically in the premolar/molar area 3 mm to the inferior border of the mandible. The full-thickness cylindrical osteotomy was performed by progressively removing the buccal cortex, tooth roots and lingual cortex, using an NSK contra-angle (1:20) handpiece with 11 mm round Medsey® trephine bur (#1315/11.0) operating at 2000 rpm under constant saline irrigation to remove the bone fragments. The lifted buccal and lingual cortex can be morselised for use as an "autograft".

Due to the heavy-load nature of the mandibular CSD model, fixation devices are required to prevent iatrogenic fracture. Therefore, a 1.5 mm and 6-hole titanium plate (MODUS®, M − 4226, Medartis AG, Switzerland) was tightly screwed (4 mm titanium screws, Medartis AG, Switzerland), in at least two holes on either side of the defect, to the border of the mandibular body (immediately beneath the defect) with a minimal influence on the defect and the space for the implantation of graft. Any remaining debris was removed from the defect with an additional 10 mL of saline irrigation. The same procedures as above were performed on the other side of the mandible. On one side, the defect was filled with BCPg scaffold or bone autograft (fragments harvested during the defect creation), while another side was left empty. The muscle and subcutaneous layers were then closed using running stitches of 3–0 Vicryl suture, and the skin was closed with interrupted stitches of 3–0 Vicryl suture. The incision closure was cleaned with Biseptine® using sterile gauze.

An outline of the surgical procedures in calvaria and mandible is illustrated in Fig. 1.

Following the surgery, each animal was kept under close surveillance until it awakened from the isoflurane anaesthesia and returned to housing. For postoperative analgesia, 0.1 mg/kg Buprevet® buprenorphine hydrochloride was administered (intramuscularly) twice per day for 3 days; and for postoperative antibiotic coverage, 5 mg/kg Baytril® enrofloxacin injectable solution was injected (subcutaneously) twice per day for 8 days. In addition, all animals were fed a soft diet for at least 7 days after surgery, followed by a regular diet of hard pellet food. Food and water were given as often as needed. The animal welfare and the surgical wounds (the swelling, signs of pain, infection, *etc.*) were assessed, and the body weights were monitored every day during the first two weeks and afterwards once per week.

2.4. Implant/bone sample collection & processing

At 4w and 12w after surgery, rabbits were sedated with an intramuscular administration of 35 mg/kg ketamine hydrochloride and 5 mg/kg xylazine hydrochloride and then euthanised by the intracardiac administration of 1 mL T61® (200 mg/mL embutramide, 50 mg/mL mebenzonium iodide, and 5 mg/mL tetracaine hydrochloride, MSD, Darmstadt, Germany). After the exposure of the calvaria defect zone, a square of 1.5 cm of the calvaria, which included a 10 mm defect site and 2.5 mm on the distal and 2.5 mm frontal side of the defect, was extracted using dental bur. The state of defect repair, as well as any abnormalities, such as dural adhesion (due to the damage of dura mater), were examined.

The whole mandible was harvested by excising the surrounding tissue, and the state of defect healing, the tooth loosening, and any abnormalities such as iatrogenic fractures, abscess at the site of the defect and intraoral communication were examined and recorded. After removing the buccal cortical titanium plate, an approximate 2 cm block of the mandible, which included the ø11 mm defect zone and 5 mm on the distal and proximal side of the defect, was extracted using dental diamond discs.

The harvested calvaria and mandible samples were immediately placed in a 10% neutral formalin solution at room temperature for 72 h, then rinsed thoroughly with running milli-Q ultrapure water before being placed in a 70% ethanol solution and were kept at 4°C before performing further analytical procedures below.

2.5. Micro-computed tomography (microCT) imaging and analysis

The above extracted mandibular and calvaria bone specimens were scanned using a microCT imaging system (Skyscan 1172, Bruker®, Kontich, Belgium) with the set parameters as follows: 100 kV, 100 A, Al + Cu filter, 1600 ms exposure time, 0.6° rotation step over 180°, frame averaging 4, pixel size 25 μm, and a field of view 1000 px by 666 px.

The following parameters were set to rebuild acquisition datasets using NRecon software (Bruker®, Kontich, Belgium) according to the manufacturer's recommendations: ring artefact reduction 5, beam hardening compensation 35%. Image grey levels range was standardised for the whole study in order to guarantee the same grey levels throughout all

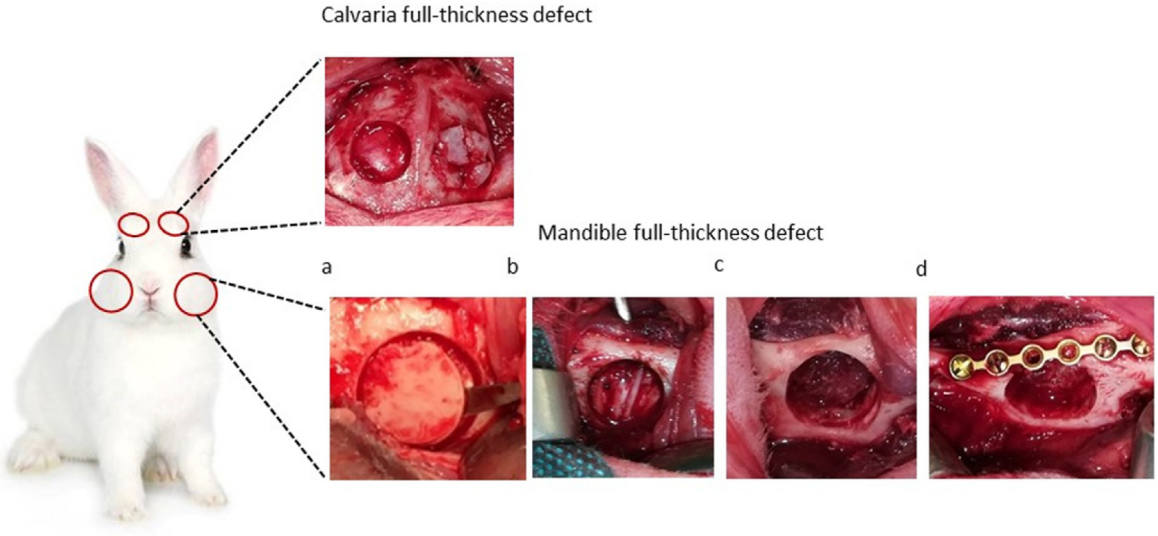

Fig. 1. Creation of bilateral calvaria (ø10 mm) and mandible (ø11mm) full-thickness defect in one rabbit: a) remove the mandible buccal cortex with a periosteal elevator after drilling with an 11 mm trephine bur, b) the exposed tooth roots, c) the view after removing the teeth and lingual cortex, d) the titanium plate was screwed at the inferior border of the mandible to prevent iatrogenic fracture.

reconstructed datasets.

For a 2D illustration of bone defects, DataViewer software (Bruker®, Kontich, Belgium) was used to reorient the reconstructed datasets: in axial cross-section view, perpendicular to the drilling axis of trephine bur, coronal suture for calvarial samples and basal edge up for mandibular samples. CTAn software (Bruker®, Kontich, Belgium) was used to evaluate the reoriented dataset. The region of interest (ROI) was defined as a 10 mm (calvaria) or 11 mm (mandible) diameter circle centred at the defect centre on the axial cross-sections, and a *reference* cross-section was determined as a median cross-section from a volume that included all bone inside the ROI. As the volume of interest (VOI), we used a total of 110 cross-sections surrounding the *reference* cross-section.

Since the high radiopacity of the BCPg ceramic is easily distinguished from that of newly formed bone, the datasets of both mandibular and calvarial BCPg sample were processed differently in order to exclude the signal of BCPg and only save that of new bone. The reoriented datasets of BCPg samples were filtered with a Gaussian filter, in contrast to that of autograft and empty samples, in which the anisotropic diffusion filter was used. Furthermore, filtered datasets of BCPg samples were binarised with Otsu algorithm to segment new bone from BCPg scaffold. On binarised datasets of BCPg samples, a dilation operation was performed to correct the high density generated by the BCPg material. The signals of BCPg scaffold thus could be removed within those dilated ROIs based on the filtered datasets.

To produce 3D models from binarised datasets, the Marching Cubes 33 approach was employed to make morphometric measurements regarding bone volume (BV, volume within the defect), tissue volume (TV, volume of the created defect) and so on. The 3D model view of bone defect can be created in CTVox software (Bruker®, Kontich, Belgium) in several positions, including both internal and external views.

2.6. Histological analysis

After the microCT scan, all samples were decalcified by immersion in a 15% EDTA solution (pH 7.2): the calvaria samples typically required 3–4 weeks to be due for tissue processing, whereas the mandibular samples generally took 2 weeks longer. After decalcification, the samples were thoroughly rinsed in 1 × PBS for 4 h to wash out remnants of the EDTA. Each mandible sample was placed separately in the cassette for tissue processing and subsequently dehydrated through a graded series of ethanol (70, 80, 90, 95, and 100 $_{v/v}$ %), and then embedded in paraffin blocks. A series of 4–5 μm thick coronal sections from the posterior, centre, and anterior of the mandible sample were performed by the microtome. The calvaria samples were sectioned at two locations: one at the defect margin, and the other at 1.5–2 mm away from the defect margin. For an in-depth characterisation of bone healing of the defect, the paraffin sections of bone tissue were stained with Masson's trichrome stain, with which the cell nuclei were stained in brown/black, collagen in green, bone in green/turquoise, the connective tissue in light green, vessels with erythrocytes in pink.

2.7. Statistical analysis

All analyses were performed with Prism v5.03.0001 (GraphPad, La Jolla, California, USA) regarding the microCT data. Results were expressed as the mean and standard deviation for each experimental group. Non-parametric analysis using Kruskal-Wallis ANOVA was used to assess the difference between the three groups. The α risk was set at 5%.

3. Results

3.1. Animal health and gross observation

Surgeries went uneventfully and there were no surgical complications. All rabbits recovered slowly but steadily started gaining weight from day 5 after the surgery and recovered good health 10–12 days after the surgery. No symptoms of infection or inflammation associated with the defect were observed over the duration of the experiment. Following the euthanasia of animals at the predetermined intervals (4w and 12w), macroscopic views of the defect sites were clean without any signs of necrosis or abscess in all rabbits, and implantation of biomaterials or autografts did not affect soft tissue healing and no intraoral communication was found.

At the calvaria defect site: in the empty group, there was only a fibrous cap associated with scattered ossified areas at both 4w and 12w; while in the autograft group, the morselised bone fragments were found to have automatically stabilised and to be well-integrated at the defect site; in the BCPg grafted defects, the granules were found to be stable and well-integrated, and still visible at 12w, which indicates a slow degradation of the BCPg during the defect-repair period.

At the mandibular defect site: no screw loosening at the titanium plate was found in any group. In the empty group, among all specimens, bone regeneration occurred to a variable degree and no solid bone union was found at 4w nor 12w; in the autograft group, the autograft fragments fused together and integrated well in all specimens at both 4w and 12w; in the BCPg group, similar to that in calvaria defect, ceramic granules were well integrated and still clearly visible at both 4w and 12w, which confirms a slow degradation of the material. In both empty and BCPg groups, the soft tissue interposition into the defect site was noticed on the lingual side of the mandible.

3.2. MicroCT qualitative and quantitative analysis of the calvarial defects

MicroCT was employed first to obtain 3D reconstruction images (Fig. 2a) for qualitatively evaluating the bone healing at the defect location. In the empty group, it showed some sparse centripetal trabecular bone formation originating from the bone edges without bone union at 4w or 12w. Only a few bone islands can be observed at 4w, starting from the edge of the defect; and at 12w, the increased number of bone islands was observed, though the defect remained incompletely healed. In the autograft group, autograft bone fragments were well integrated into the defect, and the bone bridging and solid bone union appeared at both 4w and 12w. For the BCPg group, it exhibited only sparse new bone formation (between ceramic granules), similar to that seen in the empty group.

The quantitative analysis of microCT was further performed to calculate the bone volume to tissue volume ratio (BV/TV) in each group (Fig. 2b). BV/TV in the autograft group (4w: 33.08% ± 2.05%, 12w: 47.42% ± 5.43%) was significantly higher ($p < 0.05$) than that in the empty group (4w: 12.85% ± 0.80%, 12w: 21.24% ± 3.10%)) and BCPg group (4w: 17.74% ± 2.69%, 12w: 17.09% ± 1.69%). BV/TV in the BCPg group showed a marginally higher tendency for new bone formation at 4w but remained constant, *i.e.* without any further increase until 12w. Although BCPg has exhibited space-filling capacity and osteoconductive potential, this implies the ability of this material to induce bone regeneration in the defects are quite compromised compared with autograft. To sum up, the bone healing efficacy of the autograft is well proven, and with the absence of complete defect repair in the empty group, the calvaria CSD model can be validated.

3.3. Histological findings for calvarial defects

At 4w and 12w after surgery, no obvious histological sign of inflammation infiltrates was observed in all groups (Fig. 3). In the empty group, collagen bundles with a few osteoblast cells covered the defect, a small amount of wedge-shaped bone had regenerated from the defect margin and a few bone islands surrounded by loose connective tissue at the centre of the defect were observed at both 4w and 12w. However, at 12w, the number of bone islands was relatively higher at the centre than that at 4w. In the autograft group, at both 4w and 12w, more mature osseous tissue with a much more compact structure was observed, and the graft-filled defect fully regains the contour of the original bone. Such

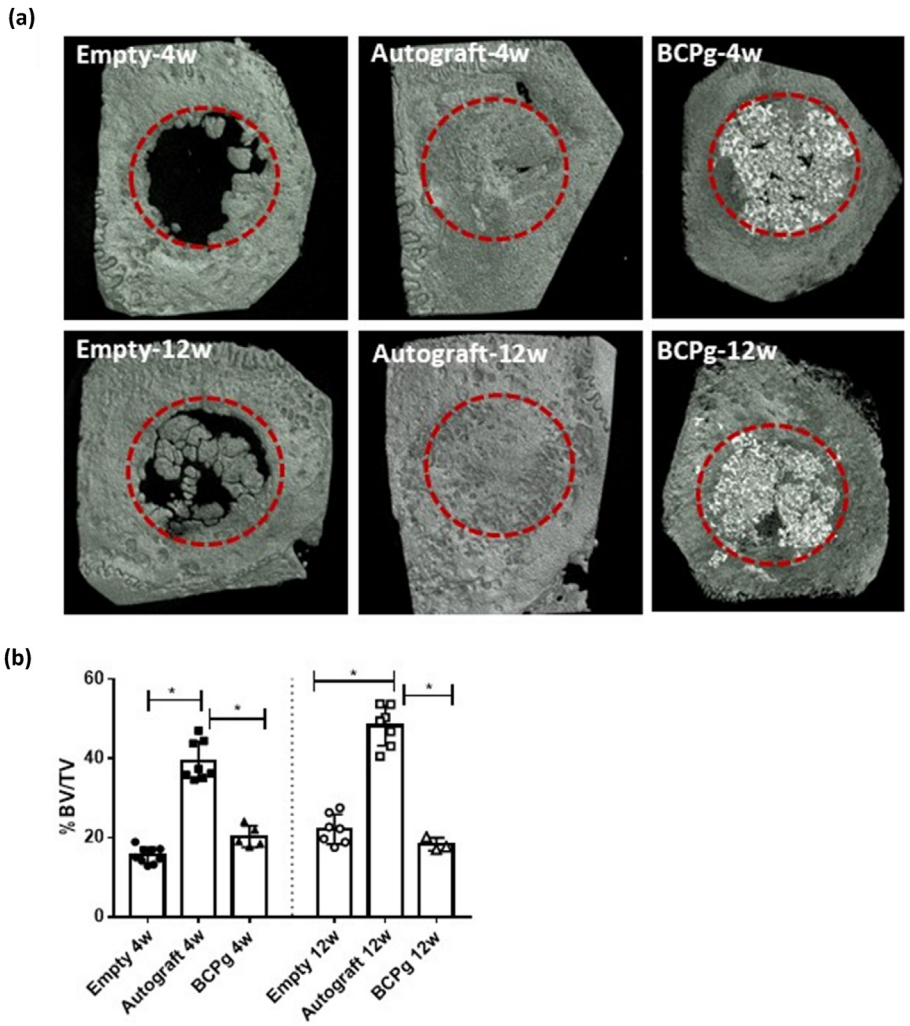

Fig. 2. MicroCT analysis of calvaria defect: a) 3D reconstruction of microCT data representatively showing the state of defect healing at 4- and 12-weeks, (b) quantitative analysis of bone volume fraction (BV/TV) at 4- and 12-weeks. Error bars indicate the mean ± standard deviation. * Indicates the statistically significant difference ($p < 0.05$) in bone-filling percentage between groups (n = 8/group): empty, autograft and BCPg (biphasic calcium phosphate granules).

histological findings were consistent with that of microCT: the 10 mm calvaria parietal defect, showing a lack of complete bone healing in the control group against the complete healing of autograft at both 4w and 12w, can be validated as a CSD model.

For the clinically relevant biomaterial group (BCPg), the ceramic material filled the space of defect well. At 4w, the newly formed bone was observed at the margin of the defect and closely around the BCPg manifesting its osteoconductive property and the osteoblasts were found in close contact with BCPg, indicating the undergoing bone-forming activities. However, most intergranular spaces were filled by loose connective tissue, not bony tissue. A similar state was found at 12w as well, except for some bony islets. Moreover, the size and the amount of BCP granules seemed to decrease as compared to that at 4w, which corresponds well to the trend found by microCT analysis: newly formed bone increasing from 4w to 12w. All findings above indicated that BCPg were well stabilised within the defect space, while new bone formation was limited: due to the space occupancy of BCPg within the defect site, inferior to that of autograft and not superior to that of the empty group.

3.4. MicroCT qualitative and quantitative analysis of mandibular defects

3D reconstruction of microCT data of mandibular defect (Fig. 4a) qualitatively showed: in the empty group, there was only sparse centripetal trabecular bone formation originating from the bone edges without any bone union at both 4w and 12w, whereas, in the autograft group, there was bone bridging and solid bone union at both 4w and 12w. Therefore, this non-union prognosis of the empty defect group in contrast to the solid bone bridge in the autograft group implies that this mandible full-thickness defect is a CSD. For the BCPg group, at both 4w and 12w, the BCP particles were well-integrated and stayed stable and, similar to that in the empty group, only sparse bone formation occurred from the edges and around the ceramic granules.

Quantitatively shown in Fig. 4b, at 4w, the BV/TV are ranked, high to low ($p < 0.05$), as the autograft group (48.30% ± 3.20%) > the empty group (32.89% ± 3.26%) > BCPg group (24.26% ± 2.66%). At 12w, the rank of BV/TV ($p < 0.05$) of three groups stays the same: the autograft group (37.8% ± 2.5%) > the empty group (23.46% ± 4.3%) > BCPg group (17.11% ± 1.6%). Thus, at both 4w and 12w, the highest amount of bone filling of defect was evidently found in the autograft group.

3.5. Histological assessment of mandibular defects

The Masson's trichrome stain on cross-sections of bone specimens, taken through the anterior, middle and posterior parts of the full-thickness defect (Fig. 5), allowed for the characterisation of post-operative healing. In the empty group, incomplete regeneration of the original bone contours at “anterior” and “posterior” defect edges was observed at both 4w and 12w, and the presence of fibrous connective

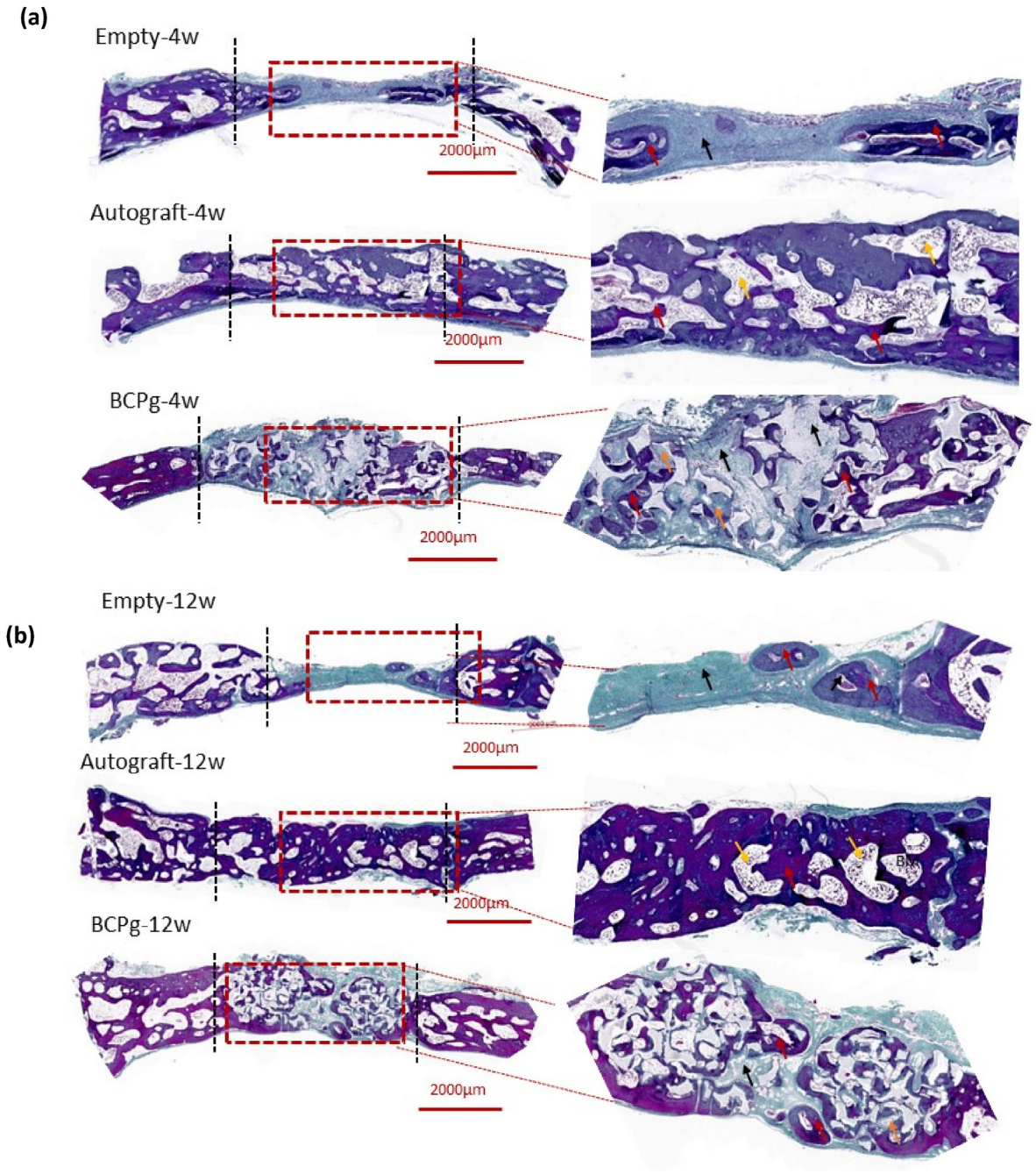

Fig. 3. Calvaria sample sections stained with Masson's trichrome stain representatively showing the defect repair in three groups: empty, autograft and BCPg (biphasic calcium phosphate granules) at a) 4 weeks and b) 12 weeks. The black dashed line denotes the defect area. The images on the right magnified the red dashed rectangular zone, showing the Red arrow (new bone), Black arrow (collagen bundles), Orange arrow (BCPg) and Yellow arrow (Bone marrow). The scale bar indicates 2000 μm.

tissue throughout the defect resulted in the lack of bone bridging in the middle of the defect, thus, even more, apparent in the "middle" cross-sections. Surprisingly, when compared to that at 4w, the amount of bone repair at 12w was slightly lower. This might be due to the fact that the new bone rapidly developed at 4w in the non-grafted defect cavity was subsequently resorbed at 12w. In contrast, in the autograft group, the bridge of cortical bone extended across the entire defect. The cortical bone graft fragments at the anterior and posterior defect margins appeared to be under the remodelling at 4w by the presence of the recruited osteoclast aligning parallel to the surface of the underlying autograft fragments and completely remodelled at 12w with less dense trabecular bone architecture in the middle.

In the BCPg group, the granules were well integrated into the defect without inducing any reaction of detrimental inflammation. At 4w, the BCPg were still clearly noticeable, mostly covered by collagenous tissue and the intergranular space was predominately occupied by loose connective tissue. Osteogenesis was observed closely around the BCP granules, showing their osteoconductive property. The newly formed bone was found in close contact with BCP granules. Bone bridging was observed mostly at the posterior and anterior defect margins, while in the middle section, the bone bridging is lacking. Similar findings were observed for bone samples at 12w. The bone regeneration at both 4w and 12w was lower than that in the empty group, which could be attributed to the delayed degradation and eventual replacement by newly formed bone.

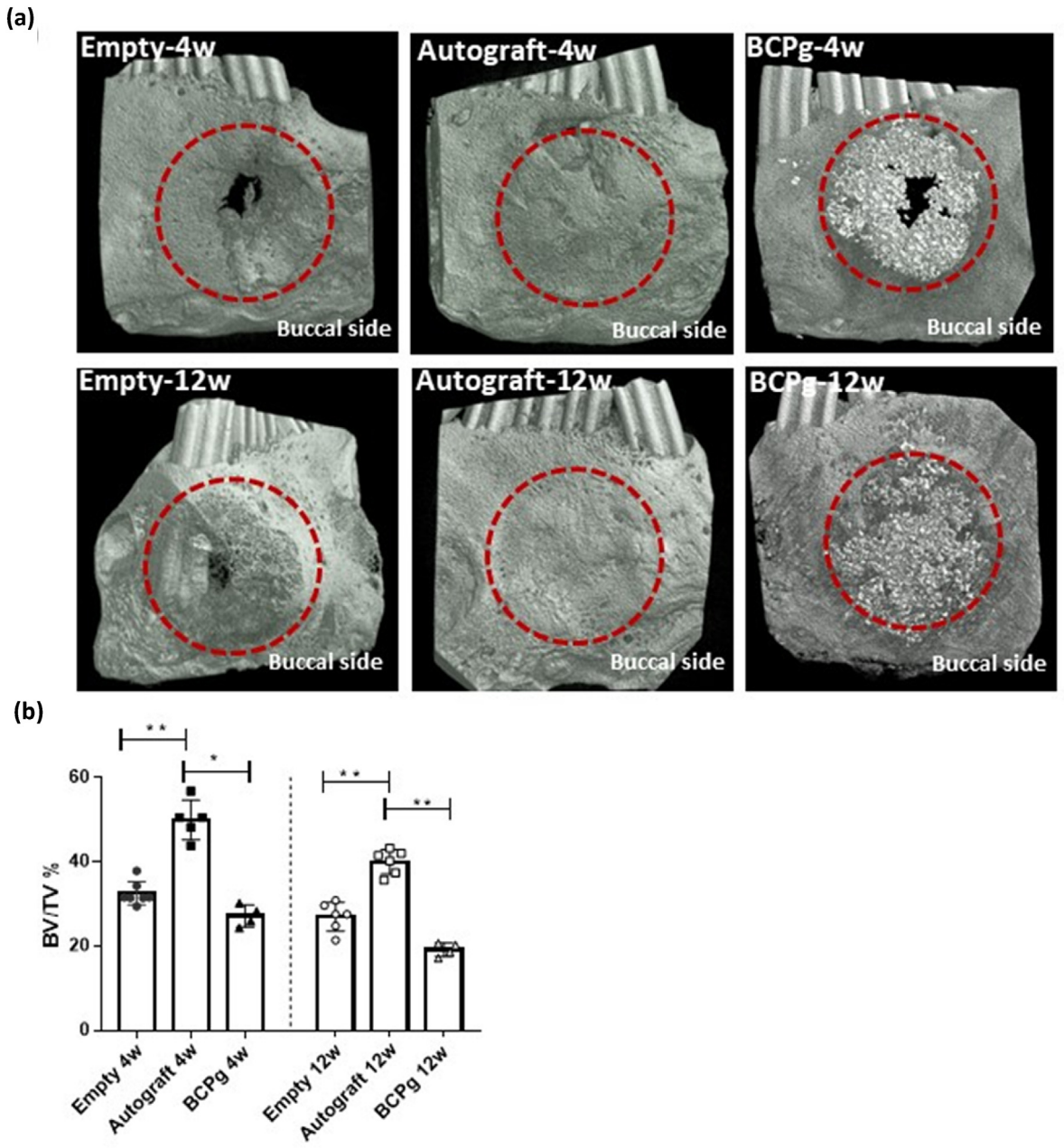

Fig. 4. MicroCT analysis of mandible defect (a) 3D reconstruction of microCT data representatively showing the state of defect healing at 4- and 12-weeks, (b) quantitative analysis of bone volume fraction (BV/TV) at 4- and 12-weeks. Error bars indicate the mean ± standard deviation. * Indicates the statistically significant difference ($p < 0.05$) in bone-filling percentage between groups (n = 8/group): empty, autograft and BCPg (biphasic calcium phosphate granules).

4. Discussion

In vitro to *in vivo* testing, and subsequently *in vivo* experiments to human trials, cannot be replicated adequately in clinical situations. This highlights how key factors are ignored when attempting to apply knowledge gained in animal experiments to clinical situations. When working toward the clinical application of any medicinal therapy product, such as a TE construct, an important step is its preclinical testing, which has been likewise recognised as a major hurdle on the way from bench to bedside. Generally, the selection of an animal model for preclinical evaluation of BSM should follow the key principles, such as the animal species, implantation site, fixation method, the implantation period and applied outcome measurement. Regarding this, the chosen bone defect models are currently a matter of massive variations, which manifests non-satisfaction with the existing models.

Rabbit allows for the preliminary biomechanical assessment and initial validation of load-bearing models among the small animals. With regard to the craniofacial region in rabbits, several studies have investigated the clinical relevance/efficacy of bone scaffolds on single-site defects, such as the calvaria, maxilla and mandible [11,15,22,23]. The mechanism of bone healing at these anatomical locations, which vary on molecular, cellular and biomechanical levels, leads to a location-dependent healing process [3]. A study by Natalina Quarto *et al.* [12] has shown that the tissue with neural crest origin has superior potential for osteogenic differentiation and osseous healing compared to that with mesodermal origin. Thus, comparison of BSMs implanted at different anatomical locations is indeed interesting for getting a global view of bone repair efficacy of material but it is difficult to be fair when the outcomes come from different animals with single-site defects, due to interindividual variability and evaluation bias. None of the studies so far

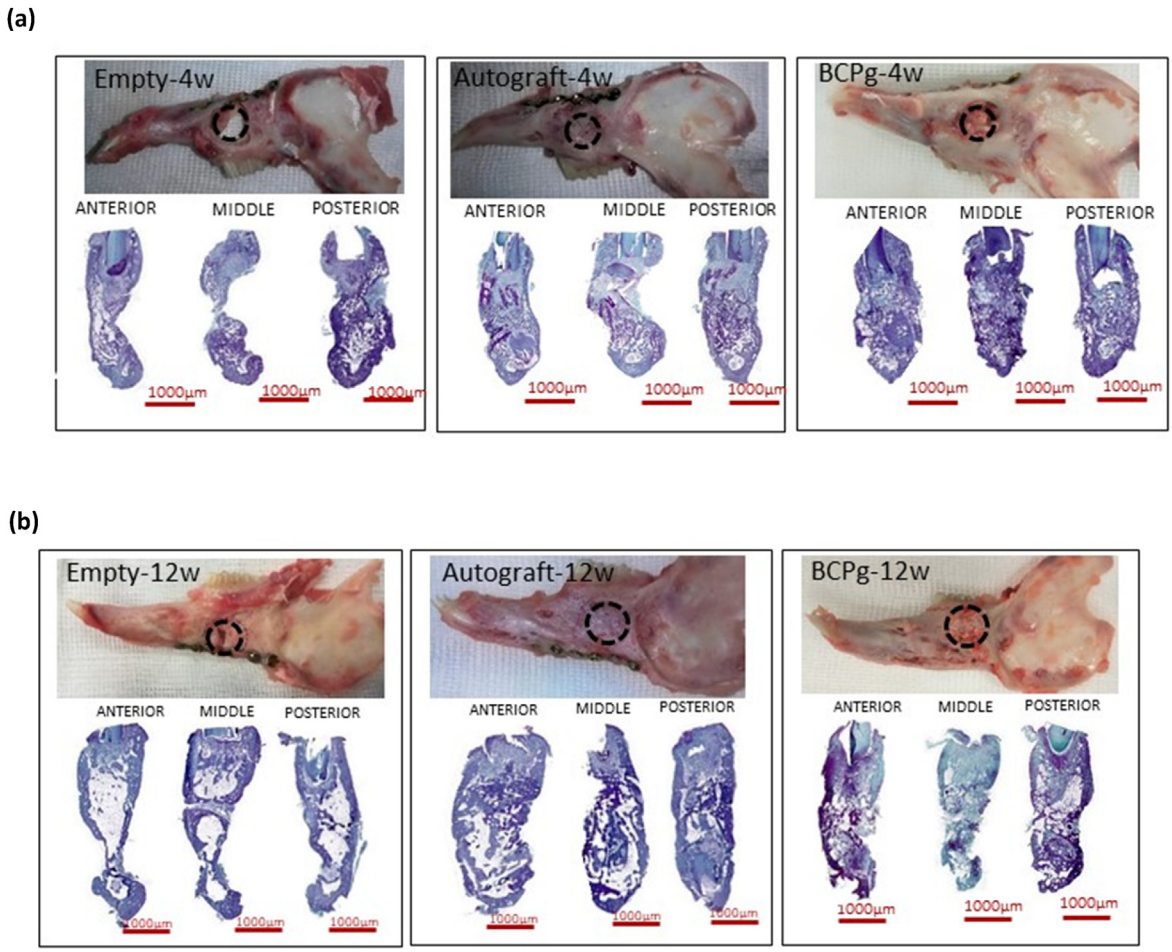

Fig. 5. Mandible sample sections stained with Masson's trichrome stain representatively showing the defect repair in three groups: empty, autograft and BCPg (biphasic calcium phosphate granules) at a) 4 weeks and b) 12 weeks. For each sample, three sections at the anterior, middle, and posterior positions of the full-thickness defect, respectively. Displayed varying amounts of trabecular and cortical bone formation at the edges of defects. The scale bar indicates 1000 μm.

investigated the efficacy of bone scaffolds in two different anatomical areas, which co-exist in the same animal [8,24–28]. For the first time, such a rabbit model was developed by this present study. The two chosen locations in this model involve the calvarial parietal defect and mandible body defect: the former is a non-loading flat bone with an embryonic paraxial mesodermal origin, whereas the latter is a load-bearing one with an embryonic origin of neural crest cells.

In addition, the size and the position of the defect are crucial factors. The existing single-site defect models have provided us with substantial data as a reference. The calvaria defect in rabbits, bilaterally placed in the parietal region with a 10 mm circular drilling hole, has been proven, by our previous study [29] and reports by others [20,25,26,28], to be CSD with limited bone healing until 12w. For the mandibular defect model, although the mandibular angle and the inferior border are the most prevalent places in the previous research [18], the former is only suitable for studying the application in a non-load-bearing area, the latter involves only loss of bone, and both avoid the loss of soft tissue or teeth. While in a load-bearing mandibular body, the anatomic structure of buccal and lingual cortex enclosing the marrow and cancellous bone, in fact, closely resembles that of the human jawbone [18]. Therefore, since we started to develop a rabbit bilateral double-site defect model in 2019, besides 10 mm calvaria parietal defects, the defects of mandible were designed at the basal edge of the mandible body as an 11 mm semi-cylindrical bicortical defect. The encouraging outcome of our previous study [29] showed, for the first time, that rabbit has a high tolerance for studied bilateral double-site CSDs. The calvaria CSD model was well validated, while the design of mandibular defect did not succeed likewise, due to the lack of facility for stabilising the graft materials in such a semi-cylindrical defect under mechanical loading, and the infectious complications from the dental lesion (odontogenic infection).

Interestingly, Shah *et al.* [29,30] reported a conventional unilateral single-site (mandible body) 10 mm cylindrical bicortical defect as a rabbit CSD model. Learning from our own lessons and inspired by the study of Shah *et al.* we modified the above semi-cylindrical defect model into a cylindrical one, without interrupting the continuity of the mandible body. In this way, the size of the defect was further enlarged with a double of the semi-cylindrical one, and it remains as a load-bearing *composite* defect model comprising the loss of bone, soft tissue and teeth. A round 11 mm (the maximum size that can be used) trephine bur is used to create a defect, which facilitates the production of a reproducible defect. However, it poses a challenge as to whether the rabbit can resist well to bilateral full-thickness mandible defects, which was never yet performed. Last but not least, the timepoints 4w and 12w were chosen for evaluating, respectively, the early phase of the healing response, such as stability of graft material and the host reaction, in addition to the late healing, such as the amount of new bone, bone resorption or bone remodelling.

For calvaria CSD, microCT and histological analyses demonstrated a statistically significant difference between the autograft and the empty group at both 4w and 12w. The obtained results from this study were totally consistent with what we reported previously [29], implying that this rabbit calvaria CSD is reproducible. For the modified mandible defect, microCT and histological analyses showed, until 12w, that the empty group had a very low degree of new bone formation at the

periphery and no bridging of the defect or regeneration of the original bony contours of the mandible. Therefore, this modified design of mandible defect (11 mm cylindrical) fully meets the criteria needed for a CSD, without showing oral communication and infection in tested animals. Moreover, the autograft fragments can be easily confined and stabilised in this defect and demonstrated full bone bridging and solid bone union at both 4w and 12w. When comparing the results of the mandible bone (cranial neural crest cells and load bearing) and the calvaria parietal bone (paraxial mesoderm cells and non-load bearing) obtained by this study, it is extremely compelling that the percentage of bone repair at 4w in mandible CSD is two times higher than in calvaria CSD, revealing the difference in osteogenesis due to their differences in embryonic origin and function.

Our study also provided a set of standard surgical procedures (performed in our lab) for a reproducible rabbit model with co-existing non-load-bearing calvaria parietal CSD and load-bearing mandibular CSD, and the methods to qualify and quantify bone regeneration within these defects and to evaluate the tissue response to biomaterial implants. Gross observation, microCT and histology are the primary techniques used in this study for analysis, however, other ancillary evaluations can also be performed to further probe *in vivo* responses to drug-releasing implants in the case, which will be applied. This experimental animal model could be a critical tool for the development and preclinical evaluation of new materials aimed at promoting tissue regeneration, as they provide evidence to the regulatory committees of whether a new product or material can be safe and efficacious in both calvaria and mandible defect setting.

Nowadays, BCP materials are definitely considered as the gold standard of BSMs in bone reconstructive surgery [7,10,21]. In this light, besides the validation of this bilateral double-site CSD model, to test the utility of which, the *in vivo* response to the BCPg was examined in this novel model. At both defect locations of our model, it highlighted good osteointegration and excellent osteoconductive properties of BCPg with evidence of the newly formed bone always in close contact with the BCPg (so-called new bone colonisation), which consists of extensive documents of BCP materials' performance in literature [7,20].

However, at both calvaria and mandible CSD, it showed minimal bone regenerative potential: the percentage of new bone formation in BCPg group was clearly inferior to the autograft, and the same as (in calvaria) or even inferior to (in the mandible) that in the empty group. Thus, the increasing new bone formation by BCP, as proven by some studies [31,32] and in numerous clinical indications, surprisingly was not shown in our model. Indeed, osteoinductive properties of BCP are still controversial in literature; even for those observations of osteoinduction using ceramics [33–37], the exact mechanism is still incompletely understood. It seems that osteoinductive properties may be dependent on the animal model. In contrast to large animal models, bone induction by BCPs is weakly observed in smaller animals. The findings on our rabbit model (small animal) also prove that no osteoinductive properties were detected from BCPg. In addition to interspecies variation, intraspecies variations have also been found [38]. From all of these, it is a real challenge to ascertain and to compare the osteoinductive potential of implanted BCP. Osteoinductive properties of BCP ceramics remain under investigation, but to date, their clinical relevance does not seem established either. As to the reason for there being less new bone formation in BCPg group at mandible CSD than that in the calvaria, it could be owing to the load-bearing property of the mandible defect. Although the musculo-aponeurotic planes opposite the graft were carefully sutured and the BCPg was well confined within the defect, the mechanical strain, generated by mastication, may impose the micromovements between BCP granules. Such micromovements and peri-implant stress impair the osseointegration process, resulting in fibrous capsule formation and subsequently slowing the new bone formation. In comparison to granular BCP, the 3D BCP customised ceramic grid used in our previous study clearly demonstrates superior stability and integration at the defect site [29].

So far, this validated double-site (calvaria and mandible) defect model, though with some limits of small animal model, fully allows for studying *in vivo* osteogenic healing ability of BSMs or TE constructs at two distinct anatomical locations in the same individual. Such comparison is much more convincing when there is no doubt from interindividual bias, not to mention other advantages, such as fairly respecting the 3Rs principle by reducing by half the number of animals used in a study with a single-site defect.

5. Conclusion

For the first time, the present study developed a standardised rabbit model that was well validated with two functionally different (non-load-bearing calvaria and load-bearing mandible) bilateral CSDs in one rabbit, which mitigates variability and enables consistent defect creation between animals. Through the application of a well-known BSM (BCPg) in this new model, it was proved adequate for evaluating the safety and efficacy of various BSMs or TE constructs and assessing the impact of tissue origin and functional differences of defect on their bone healing capabilities, while minimising heterogeneity derived from interindividual variability and the evaluation bias.

Credit author statement

Sindhu Kotagudda Ranganath: Methodology, Interpretation of data, Writing – original draft preparation, Reviewing. **Matthias Schlund**: Methodology, Reviewing. **Jerome Delattre**: Data Acquisition. **Joel Ferri**: Conceptualization, Reviewing. **Feng Chai**: Conceptualization, Methodology, Interpretation of data, Writing- Reviewing and Editing.

Declaration of competing interest

The authors declare the following financial interests/personal relationships which may be considered as potential competing interests: Feng Chai reports financial support was provided by European Union.

Acknowledgement

The authors would like to thank the Platform Experimental Resources, D.H.U.R.E, University of Lille, for their support on animal studies. We also thank Mrs A-S. Drucbert for her technical help in histological analysis. It was supported by the cross-border INTERREG "North-West Europe" fund BONE 2014–2020.

References

[1] S. Zeiter, K. Koschitzki, M. Alini, F. Jakob, M. Rudert, M. Herrmann, Evaluation of preclinical models for the testing of bone tissue-engineered constructs, Tissue Eng. C Methods 26 (2) (2020) 107–117.
[2] S.L. Piotrowski, L. Wilson, N. Dharmaraj, A. Hamze, A. Clark, R. Tailor, et al., Development and characterization of a rabbit model of compromised maxillofacial wound healing, Tissue Eng. C Methods 25 (3) (2019) 160–167.
[3] D. Wang, J.R. Gilbert, X. Zhang, B. Zhao, D.F.E. Ker, G.M. Cooper, Calvarial versus long bone: implications for tailoring skeletal tissue engineering, Tissue Eng. B Rev. 26 (2020) 46–63. Mary Ann Liebert Inc.
[4] L.M. Wancket, Animal models for evaluation of bone implants and devices: comparative bone structure and common model uses, Vet. Pathol. 52 (5) (2015) 842–850. Sep. 24.
[5] L.M. Atayde, P.P. Cortez, T. Pereira, P.A.S. Armada-Da-Silva, A. Afonso, M.A. Lopes, et al., A new sheep model with automatized analysis of biomaterial-induced bone tissue regeneration, J. Mater. Sci. Mater. Med. 25 (8) (2014) 1885–1901.
[6] A. Kengelbach-Weigand, C. Thielen, T. Bäuerle, R. Götzl, T. Gerber, C. Körner, et al., Personalized medicine for reconstruction of critical-size bone defects – a translational approach with customizable vascularized bone tissue, npj Regen. Med. 6 (1) (2021).
[7] E.U. Lee, D.J. Kim, H.C. Lim, J.S. Lee, U.W. Jung, S.H. Choi, Comparative evaluation of biphasic calcium phosphate and biphasic calcium phosphate collagen composite on osteoconductive potency in rabbit calvarial defect, Biomater. Res. 19 (1) (2015) 1–7.

[8] P. Pripatnanont, T. Nuntanaranont, S. Vongvatcharanon, K. Phurisat, The primacy of platelet-rich fibrin on bone regeneration of various grafts in rabbit's calvarial defects, J. Cranio-Maxillofacial Surg. 41 (8) (2013). Dec.
[9] N. Wongsupa, T. Nuntanaranont, S. Kamolmattayakul, N. Thuaksuban, Assessment of bone regeneration of a tissue-engineered bone complex using human dental pulp stem cells/poly(ε-caprolactone)-biphasic calcium phosphate scaffold constructs in rabbit calvarial defects, J. Mater. Sci. Mater. Med. 28 (5) (2017). May 1.
[10] M. Leventis, P. Fairbairn, C. Mangham, A. Galanos, O. Vasiliadis, D. Papavasileiou, et al., Bone healing in rabbit calvaria defects using a synthetic bone substitute: a histological and micro-CT comparative study, Materials 11 (10) (2018) 1–13.
[11] V.-E. Campillo, S. Langonnet, A. Pierrefeu, A.-G. Chaux-Bodard, Anatomic and histological study of the rabbit mandible as an experimental model for wound healing and surgical therapies, Lab. Anim. 48 (4) (2014) 273–277. Oct 20.
[12] N. Quarto, D.C. Wan, M.D. Kwan, N.J. Panetta, S. Li, M.T. Longaker, Origin matters: differences in embryonic tissue origin and Wnt signaling determine the osteogenic potential and healing capacity of frontal and parietal calvarial bones, J. Bone Miner. Res. 25 (7) (2010) 1680–1694.
[13] T. Taguchi, J. Watahiki, T. Nampo, Y. Ichikawa, G. Yamamoto, M. Sakurai, et al., The usefulness of mandibular and maxillary bone derived from neural crest as bone graft substitutes, Showa Univ. J. Med. Sci. 28 (3) (2016) 241–248.
[14] J.C. Zhang, H.Y. Lu, G.Y. Lv, A.C. Mo, Y.G. Yan, C. Huang, The repair of critical-size defects with porous hydroxyapatite/polyamide nanocomposite: an experimental study in rabbit mandibles, Int. J. Oral Maxillofac. Surg. 39 (5) (2010) 469–477. May.
[15] R.E. Hayden, D.P. Mullin, A.K. Patel, Reconstruction of the segmental mandibular defect: current state of the art, in: Current Opinion in Otolaryngology and Head and Neck Surgery, vol. 20, Curr Opin Otolaryngol Head Neck Surg, 2012, pp. 231–236.
[16] J.P. Schmitz, J.O. Hollinger, The critical size defect as an experimental model for craniomandibulofacial nonunions, Clin. Orthop. Relat. Res. 205 (1986) 299–308.
[17] Y. Li, S.K. Chen, L. Li, L. Qin, X.L. Wang, Y.X. Lai, Bone defect animal models for testing efficacy of bone substitute biomaterials, J. Orthopaedic Transl. 3 (2015) 95–104. Elsevier (Singapore) Pte Ltd.
[18] G. Cheng, Z. Li, Q. Wan, K. Lv, D. Li, X. Xing, et al., A novel animal model treated with tooth extraction to repair the full-thickness defects in the mandible of rabbits, J. Surg. Res. 194 (2) (2015) 706–716.
[19] J.Z. Baskin, B.M. White, A. Vasanji, T.E. Love, S.J. Eppell, Mandible biomechanics and continuously erupting teeth: a new defect model for studying load-bearing biomaterials, Biomedicines 9 (7) (2021) 1–20.
[20] J.-C. Park, H.-C. Lim, J.-Y. Sohn, J.-H. Yun, U.-W. Jung, C.-S. Kim, et al., Bone regeneration capacity of two different macroporous biphasic calcium materials in rabbit calvarial defect, J. Korean Acad. Periodontol. 39 (Suppl) (2009) 223.
[21] D. Wang, A. Tabassum, G. Wu, L. Deng, D. Wismeijer, Y. Liu, Bone regeneration in critical-sized bone defect enhanced by introducing osteoinductivity to biphasic calcium phosphate granules, Clin. Oral Implants Res. 28 (3) (2017) 251–260.
[22] G.I. Brierly, S. Tredinnick, A. Lynham, M.A. Woodruff, Critical sized mandibular defect regeneration in preclinical in vivo models, Curr. Mol. Biol. Rep. 2 (2) (2016) 83–89. Jun 18.
[23] H. Jianqi, H. Hong, S. Lieping, G. Genghua, Comparison of calcium alginate film with collagen membrane for guided bone regeneration in mandibular defects in rabbits, J. Oral Maxillofac. Surg. 60 (12) (2002) 1449–1454. Dec 1.
[24] G. Cheng, Z. Li, Q. Wan, K. Lv, D. Li, X. Xing, et al., A novel animal model treated with tooth extraction to repair the full-thickness defects in the mandible of rabbits, J. Surg. Res. 194 (2) (2015) 706–716. Apr 1.
[25] K.G. Lee, K.S. Lee, Y.J. Kang, J.H. Hwang, S.H. Lee, S.H. Park, et al., Rabbit calvarial defect model for customized 3D-printed bone grafts, Tissue Eng. C Methods 24 (5) (2018) 255–262. May 1.
[26] R.A. Delgado-Ruiz, J.L. Calvo-Guirado, G.E. Romanos, Critical size defects for bone regeneration experiments in rabbit calvariae: systematic review and quality evaluation using ARRIVE guidelines, Clin. Oral Implants Res. 26 (8) (2015) 915–930. Aug 1.
[27] L. da Costa Oliveira, A.F. Giovanini, A. Abuabara, L.G. Klug, C.C. Gonzaga, J.C. Zielak, et al., Fragmented adipose tissue graft for bone healing: histological and histometric study in rabbits' calvaria, Med. Oral Patol. Oral Cir. Bucal 18 (3) (2013). May.
[28] J.Y. Sohn, J.C. Park, Y.J. Um, U.W. Jung, C.S. Kim, K.S. Cho, et al., Spontaneous healing capacity of rabbit cranial defects of various sizes, J. Periodontal Implant Sci. 40 (4) (2010) 180–187. Aug.
[29] M. Schlund, A. Depeyre, S.K. Ranganath, P. Marchandise, F. Chai, J. Ferri, Rabbit calvarial and mandibular critical-sized bone defects as an experimental model for the evaluation of craniofacial bone tissue regeneration, J. Stomatol. Oral Maxillofac Surg. (2021).
[30] S.R. Shah, S. Young, J.L. Goldman, J.A. Jansen, M.E. Wong, A.G. Mikos, A composite critical-size rabbit mandibular defect for evaluation of craniofacial tissue regeneration, Nat. Protoc. 11 (10) (2016) 1989–2009. Oct 1.
[31] L.E. Ung, K.D. Ju, H.C. Lim, J.S. Lee, U.W. Jung, S.H. Choi, Comparative evaluation of biphasic calcium phosphate and biphasic calcium phosphate collagen composite on osteoconductive potency in rabbit calvarial defect, Biomater. Res. 19 (1) (2015).
[32] P.S. Santos, T.M. Cestari, J.B. Paulin, R. Martins, C.A. Rocha, R.V.N. Arantes, et al., Osteoinductive porous biphasic calcium phosphate ceramic as an alternative to autogenous bone grafting in the treatment of mandibular bone critical-size defects, J Biomed Mater Res - Part B Appl Biomater. 106 (4) (2018) 1546–1557. May 1.
[33] H. Yuan, J.D. De Bruijn, Y. Li, J. Feng, Z. Yang, K. De Groot, et al., Bone formation induced by calcium phosphate ceramics in soft tissue of dogs: a comparative study between porous α-TCP and β-TCP, J. Mater. Sci. Mater. Med. 12 (1) (2001) 7–13.
[34] H. Yuan, J.D. De Bruijn, X. Zhang, C.A. Van Blitterswijk, K. De Groot, Bone induction by porous glass ceramic made from Bioglass® (45S5), J. Biomed. Mater. Res. 58 (3) (2001) 270–276.
[35] P. Habibovic, U. Gbureck, C.J. Doillon, D.C. Bassett, C.A. van Blitterswijk, J.E. Barralet, Osteoconduction and osteoinduction of low-temperature 3D printed bioceramic implants, Biomaterials 29 (7) (2008) 944–953.
[36] H. Yuan, Y. Li, J. De Bruijn, K. De Groot, X. Zhang, Tissue responses of calcium phosphate cement: a study in dogs, Biomaterials 21 (12) (2000) 1283–1290.
[37] F. Zhao, Z. Yang, L. Liu, D. Chen, L. Shao, X. Chen, Design and evaluation of a novel sub-scaffold dental implant system based on the osteoinduction of micro-nano bioactive glass, Biomater. Transl. 1 (1) (2020) 82–88.
[38] W.F. Daamen, J.H. Veerkamp, J.C.M. van Hest, T.H. van Kuppevelt, Elastin as a biomaterial for tissue engineering, Biomaterials 28 (30) (2007) 4378–4398.